SRC-TR-87-89

CHEMICAL PROCESS SYSTEMS LABORATORY

The Dispersion of Viscous Liquids by Turbulent Flow in a Static Mixer

by

Paul D. Berkman
Richard V. Calabrese

RESEARCH REPORT

CHEMICAL PROCESS SYSTEMS ENGINEERING LABORATORY

THE DISPERSION OF VISCOUS LIQUIDS BY TURBULENT FLOW IN A STATIC MIXER

Paul D. Berkman and Richard V. Calabrese

A CONSTITUENT LABORATORY OF THE SYSTEMS RESEARCH CENTER

THE UNIVERSITY OF MARYLAND
COLLEGE PARK, MARYLAND 20742

THE DISPERSION OF VISCOUS LIQUIDS BY TURBULENT FLOW IN A STATIC MIXER

by

Paul D. Berkman and Richard V. Calabrese
Department of Chemical and Nuclear Engineering
University of Maryland, College Park, MD 20742

Submitted to:
AICHE Journal
MS No. 86P00454

Keywords: Liquid-Liquid Dispersion, Static Mixer, Drop Size Distribution, Turbulent Liquid-Liquid Contacting

---

Correspondence concerning this paper should be directed to R. V. Calabrese

P. D. Berkman is presently with Naval Ordinace Station, Indian Head, MD.

ABSTRACT

Drop are stabilized in agitated liquid-liguid systems by both surface and internal viscous forces. The dispersion of an inviscid liquid into a turbulent continuous phase in static mixers has been studied but the effect of dispersed phase viscosity is not well understood. Systemmatic experiments have been conducted in a Kenics mixer by photographically examining dilute suspensions of viscous oils in water to determine how viscosity and conditions of agitation affect equilibrium mean drop size and size distribution. A semi-empirical theory is developed which correlates the mean size data and collapses to the well-known Weber No. result in the inviscid limit. A correlation for drop size distribution in terms of cumulative volume frequency is developed by normalization with D_{32}. Measurements at the mixer entrance indicate that the method of introduction of the dispersed phase should be considered when evaluating mixer performance.

INTRODUCTION

While the determination of interfacial area for liquid-liquid dispersions produced in turbulent stirred tank contactors has commanded considerable attention (Tavlarides and Stamatoudis, 1981), few studies have focused upon continuous, inline mixers. Yet static mixers offer an attractive alternative to stirred vessels due to narrower residence time distribution, lower capital and operating costs, and minimal maintenance requirements.

Middleman (1974) measured drop size distributions in Kenics mixers by producing dilute suspensions of six different organic liquids in water. He found that equilibrium was achieved after about $n_e = 10$ mixer elements. For inviscid dispersed phases ($\mu_d \leq 1$ mPa·s) the equilibrium data were well correlated by

$$\frac{D_{32}}{D_o} = A\, We^{-3/5} \qquad (1)$$

where $We = \rho_c \bar{v}^2 D_o/\sigma$ is the system Weber No. Middleman derived Eq.1 by assuming that the disruptive energy acting upon a drop was due to inertial subrange eddies and that drop stability was due only to interfacial tension. A slight dependency on Reynolds No. resulted and was ignored. As expected, Eq. 1 failed to correlate his data for $5 \leq \mu_d \leq 26$ mPa·s. Equilibrium drop size distributions were found to be normally distributed in volume and were correlated by normalization with D_{32}. Additional data for benzene-water dispersions ($\mu_d = 0.6$ mPa·s) showed that mean drop diameter was independent of dispersed phase volume fraction for $0.01 < \Phi < 0.25$.

Chen and Libby (1978) dispersed kerosene and mineral oil in water in a Kenics mixer. They correlated mean drop size data, empirically, in terms of Weber No. and viscosity ratio. A single drop size distribution was reported. Al Taweel and Walker (1983) measured mean drop size for dilute dispersions of kerosene in water in two different configurations of a Lightnin "In-liner" mixer. They systematically varied energy dissipation rate (average velocity) and the number of mixer elements (residence

time). They reported the number of elements required to achieve equilibrium and found that their data could be correlated in terms of energy dissipation rate or Weber No. A quantitative measure of dispersion efficiency was also given.

This study extends previous work by examining the extent to which internal viscous resistance to breakage affects equilibrium mean drop size and drop size distribution for turbulent flow through a static mixer. Mixer performance is evaluated from photographic observations of drop size at the entrance and exit of a 24 element Kenics mixer. Systematic experiments for dilute suspensions of various oils ($0.63 \leq \mu_d \leq 204$ mPa·s) in water indicate that equilibrium mean drop size increases and the size distriubtion broadens with increasing dispersed phase viscosity and decreasing Reynolds No. (or energy dissipation rate).

Eq. 1 is extended via mechanistic arguments to include the effect of dispersed phase viscosity. Mean drop size is shown to depend on two system parameters: the Weber No. and a Viscosity Group, Vi, representing the ratio of dispersed phase viscous to surface forces. The two geometric constants in the resulting semi-empirical equation are obtained from linear regression of the data. In the inviscid limit this correlation provides an equally good fit to the low viscosity dispersed phase data of Middleman (1974).

Equilibrium drop sizes are found to be normally distributed in volume. A correlation which applies to both inviscid and viscous dispersed phases is developed via non-linear least squares regression by normalization of the cumulative volume frequency data with D_{32}. A comparison of size distributions at the entrance and exit of the mixer indicates that the method of introduction of the dispersed phase should be considered when evaluating mixer performance.

The effect of system variables on and the form of the correlations for equilibrium mean drop size and size distribution are found to be the same as for turbulent stirred tank contactors.

EXPERIMENTAL

The single 24 element, 1.91 cm diameter stainless steel Kenics mixer used in this study has a pitch (L_e/D_o) of 1.5. Although Middleman's (1974) data indicate that only 10 elements are required to achieve equilibrium, this much longer mixer was selected since considerably more viscous dispersed phases are employed here. Although the effect of μ_d on time (distance) to reach equilibrium is unknown, it is prudent to assume that its effect is to increase said time.

A schematic diagram of the experimental facility is given in Figure 1. Water is fed from a 120 liter constant head tank through 15.2 cm diameter PVC pipe to a point below the test section. It then passes through a U bend and reducer so that it becomes directed vertically upward through a 1.91 cm ID clear acrylic tube. The bell shaped reducer is designed to minimize flow disturbances at the tube entrance. The test section is located in the acrylic tube with the mixer entrance at 50 tube diameters downstream from the reducer. The flow exiting the mixer passes through a metering valve and a flexible hose and then into a collecting tank for discharge to a drain. The volumetric flow rate was obtained by moving the discharge of the flexible hose to a large glass cylinder and measuring the time required to collect 20 liters of water. An available precision mass flow meter could not be used due to excessive pressure drop. The pressure drop across the mixer was measured with static head tubes connected to pressure taps in the wall of the test section.

Filtered water was supplied to the constant head tank form the building water supply. As a result, it was difficult to control water temperature. However, water and room temperature did not differ substantially and remained constant during any given run. We therefore accepted a several degree seasonal temperature variation to avoid complications associated with avoiding recirculation of and ultimate removal of the dispersed phase from a more controllable closed loop system.

The dispersed phase was introduced through a 0.25 cm I.D., 0.32 cm O.D. stainless steel injector tube which passes through the acrylic tube wall and makes a 90°C turn so that its vertical leg is concentric to the axis of the acrylic tube. The vertical leg is 15 tube diameters long with its exit located about 9 cm below the mixer entrance to insure that drops produced by it relax to a spherical shape before entering the mixer. The injector tube is fed by gas pressure from a 1.5 liter stainless steel reservoir. The flow rate is regulated by a calibrated metering valve.

Small square, water-filled plexiglas boxes surrounding the test section were used to eliminate optical distortion while photographing the dispersion. The initial drop size distribution was acquired just below the mixer entrance. The final distribution was measured about 10 cm above the mixer exit. This distance was required to allow exiting oil globules to relax to a spherical shape. Photographs were taken with a Nikon F3 35 mm SLR camera system equipped with a MD-4 motor drive, a PB-6 bellows and a fully retracted, reverse mounted 55 mm micro-Nikor lens. Magnifications from 1.5 to 3 times actual size were achieved by adjustment of the bellows. In this configuration the depth of field is so small that parallax errors are negligible and the magnification is solely determined by the bellows setting (focal distance). Illumination was provided by a Sunpak 611 automatic thyristor flash placed directly opposite the camera lens. The manually set flash duration of one-thirty thousand seconds was sufficiently fast to freeze droplet motion.

Drop sizes were measured from the negatives (Kodak Technical Pan Film 2415) using a semi-automated digitizing facility described by Wang and Calabrese (1986). Initial drop size distributions were determined from at least 100 counts of drop size (>50 frames of film). Final drop size distributions were determined from at least 300 counts (>25 frames). Sauter mean diameter was calculated from

$$D_{32} = \sum_{i=1}^{n} D_i^3 \Big/ \sum_{i=1}^{n} D_i^2 \qquad (2)$$

Cumulative volume frequency was calculated from

$$F_v(D_i) = \sum_{J=1}^{i} D_j^3 \Big/ \sum_{J=1}^{n} D_j^3 \qquad (3)$$

Seven different dispersed phase fluids were employed. Physical properties are given in Table 1 for the temperatures at which experiments were performed. Each oil is assigned a nominal viscosity, μ_d', to facilitate subsequent discussion. Viscosities were measured with calibrated Cannon-Fenske viscometers and densities with precision hydrometers. Interfacial tensions with filtered building water were measured via a du Noüy ring technique (Calabrese and Wang, 1986). Handbook data were used for the density and viscosity of water. Table 1 shows that a wide range of dispersed phase viscosity was considered. A more limited range of interfacial tension was employed since its role has been systematically studied by Middleman (1974).

For each dispersed phase, experiments were conducted at pipe Reynolds numbers of 12000, 15000, 18000 and 21000 by fine adjustment of water flow rate to compensate for run to run temperature variations. The Reynolds No. is based upon the average velocity of the continuous phase ($0.58 < \bar{V} < 1.05$ m/sec) since dispersed phase volume fractions were too small to affect total flow rate.

The constraints placed upon the oil injector were to produce large drops of narrow size distribution at a dispersed phase hold-up of less than 0.1% by volume for the specified pipe Reynolds No. This proved to be extremely difficult to achieve. The injector flow may be viewed as a capillary jet discharging into a coflowing turbulent stream, a system for which design data are lacking. Initial experiments with different diameter capillary tubes revealed that the action of the surrounding turbulence dictated the use of the selected injector tube at

minimum discharge velocity. For each run the injector flow rate was adjusted while visually observing the capillary jet with the aid of a strobe light to achieve an acceptable result. Therefore, actual holdups ranged from $0.00057 \leq \Phi \leq 0.001$. Nevertheless, it was necessary to accept the presence of some small satellite droplets, particularly for the more viscous oils, and to account for their presence in evaluating mixer performance. It was indeed these concerns that motivated us to measure initial drop size.

RESULTS

The pressure drop measurements were converted to Fanning friction factors (Bird, et.al., 1960) via

$$\Delta P = \frac{4L}{D_o} \quad \frac{1}{2} \quad \rho_c \bar{V}^2 \quad f \tag{4}$$

The results, given in Figure 2, show that the friction factor is constant ($f = 0.416$) for $Re \geq 12{,}000$ and is about 50 times greater than those for a smooth pipe. Middleman (1974) assumed that friction factors for Kenics mixers showed a Reynolds No. dependency similar to that for a smooth pipe. These data show a stronger analogy to a rough pipe. Mean energy dissipation rates may be estimated from:

$$\bar{\varepsilon} = \frac{\bar{V} \ \Delta P}{\rho_c \ L} \tag{5}$$

which combined with Eq. 4 yields

$$\bar{\varepsilon} = \frac{2 \ \bar{V}^3 \ f}{D_o} \tag{6}$$

An estimate of the Kolmogorov microscale is given by

$$\bar{\eta} = \left(\nu_c^3 / \bar{\varepsilon} \right)^{\frac{1}{4}} \tag{7}$$

With Eq. 6 and the definition $Re = \bar{V} D_o / \nu_c$, Eq. 7 yields

$$\bar{\eta} = \left(\frac{D_o^4}{2\ f\ Re^3} \right)^{\frac{1}{4}} \qquad (8)$$

Using Eqs. (6) and (8) shows that for this study, the range 12000 < Re < 21000 corresponds to 8.5 < $\bar{\varepsilon}$ < 50.5 m^2/s^3 and 17.4 > $\bar{\eta}$ > 11.5 μm, respectively.

Initial and final Sauter mean diameters for each experiment are given in Table 2. Typical initial and final drop size distributions are given in Figures 3 to 5.

It is not the purpose of this study to provide a detailed analysis of drop sizes produced by breakup of a capillary jet discharged into a turbulent environment. However, some attention must be given to the initial size distribution to insure that our analysis of mixer performance is physically meaningful.

Table 2 shows that initial Sauter mean diameter increases with increasing dispersed phase viscosity and decreasing Reynolds No. A comparison of the 50 mPa·s silicone oil and 45 mPa·s paraffin oil data indicates an increase in D_{32} with interfacial tension. The effect of μ_d and σ on final D_{32} is similar. However, final mean diameters decrease much more rapidly with Re. As a result, the ratio of initial to final D_{32} increases with Re and decreases with μ_d. In any event, this ratio varies from about 3 to 8 over the range of experiments. A question therefore arises concerning the influence of initial drop size on mixer performance. The extent of such influence is best understood by examining drop size distribution.

Figure 3 shows that at low μ_d, there is a finite but small overlap between initial and final drop sizes. The initial distributions are broader with maximum overlap occuring at lower Re. However, only a small portion of the initial volume is affected; that is, less than 1% of the initial volume of dispersed phase entering the mixer is in drops which may not experience breakage. It is therefore reasonable to assume that the final distribution, with the possible exception of the large size tail, is independent of conditions at the mixer entrance.

Figure 4 shows a less satisfactory situation at higher μ_d. Initial distributions are much broader. At low Re, as much as 2% of the drop volume entering the mixer may not experience breakage. Figure 5 reveals that for the high viscosity paraffin oil, the initial distribution is bimodal, containing many small satellite droplets and a fairly narrow distribution of daughters (larger drops). As much as 4% of the initial drop volume may not experience breakage, thereby contributing to the large size tail of the final drop size distribution.

Despite these findings, it is reasonable to assume that drop sizes at the mixer exit are representative of mixer performance. It is possible that a drop slightly larger than D_{max}, entering this very long mixer, may not have sufficient time to break. However, such errors are tolerable given other errors inherent in the experimental procedure. Furthermore, the small volumes involved should not significantly affect the determination of final D_{32}. It is prudent, however to consider the effect of initial drop size on the large size tail of the final size distribution, particularly at low Re and high μ_d.

Figure 6 is a plot of final Sauter mean diameter versus dispersed phase viscosity at constant interfacial tension. Reynolds No. is a parameter. D_{32} is seen to increase almost linearly with μ_d and to decrease with Re (or $\bar{\epsilon}$). Figure 7 shows the relationship between Sauter mean diameter and maximum stable drop size at the mixer exit. The data are well correlated by

$$D_{max} = 1.5\ D_{32} \qquad (9)$$

A similar result was found by Calabrese et. al. (1986) and Wang and Calabrese (1986) in stirred tanks for the same physical property range. These authors argued mechanistically for such a relationship. The same arguments can be applied here.

Figures 3 to 5 show that the final drop size distribution exhibits almost straightline behavior on normal probability coordinates and is therefore about normally distributed in volume. The distribution broadens with decreasing Re (or $\bar{\epsilon}$) and

increasing μ_d. Figure 8 provides a more convincing argument for the effect of dispersed phase viscosity since these paraffin oil data are presented at constant Re and σ. The effects of dispersed phase viscosity and conditions of agitation on final drop size distribution are similar to those found by Calabrese et. al. (1986) and Wang and Calabrese (1986) in stirred tanks.

MEAN DROP SIZE CORRELATION

A mechanistic model for maximum stable drop size can be developed by equating the turbulent disruptive force acting upon the drop to the cohesive forces due to surface and internal viscous resistance to breakage. For $D = D_{max}$

$$\tau_c = C_1 \frac{\sigma}{D} + C_2 \frac{\mu_d}{D} \left(\tau_c / \rho_d \right)^{\frac{1}{2}} \qquad (10)$$

Eq. 10 is consistent with arguments put forth by Kolmogorov (1949) and Hinze (1955). It is the same as that used by Hughmark (1971) to correlate the data of Sleicher (1962) and Paul and Sleicher (1965) for turbulent pipe flow and by Calabrese et.al. (1986) to correlate their data for turbulent stirred tanks. Recently, Davies (1985) has argued that the form of Eq. 10 applies to a variety of turbulent emulsifiers.

In static mixers, the largest eddies are of order of 0.5 D_o while the smallest eddies are of order $\bar{\eta}$. The data of Figure 7 show that for the conditions of this study, maximum stable drop sizes are much larger than the microscale (reported earlier) but much smaller than the macroscale. These are the conditions for which Kolmogorov's theory for the inertial subrange applies, and τ_c is given by (Shinnar, 1961)

$$\tau_c = 1.5\alpha \rho_c \varepsilon^{2/3} D^{2/3} \qquad (11)$$

It is further assumed, following Chen and Middleman (1967) and Middleman (1974), that the local energy dissipation rate, ε, can be related to the mean energy dissipation rate, $\bar{\varepsilon}$, by a constant

for geometrically similar systems. With $\varepsilon = C_3 \bar{\varepsilon}$, Eqs. 10 and 11 can be combined to yield

$$D_{max} = C_4 \left(\frac{\sigma}{\rho_c \bar{\varepsilon}^{2/3}} \right)^{3/5} \left[1 + C_5 \frac{\mu_d \bar{\varepsilon}^{1/3} D_{max}^{1/3}}{\sigma} \left(\frac{\rho_c}{\rho_d} \right)^{1/2} \right]^{3/5} \quad (12)$$

For dilute suspensions, Eq. 12 can be combined with Eqs. 6 and 9 to yield

$$\frac{D_{32}}{D_o} = C_6 We^{-3/5} f^{-2/5} \left[1 + C_7 f^{1/3} Vi \left(\frac{D_{32}}{D_o} \right)^{1/3} \right]^{3/5} \quad (13)$$

where $V_i = (\mu_d \bar{V}/\sigma)(\rho_c/\rho_d)^{\frac{1}{2}}$ is a viscosity group or capillary number representing the ratio of viscous to surface forces acting to stabilize the drop. Sleicher (1962) correlated his pipe flow data by arguing for such a viscosity group on physical grounds.

For the static mixer of this study f is constant for Re>12,000. Therefore, for the data reported here, Eq. 13 reduces to

$$\frac{D_{32}}{D_o} = A We^{-3/5} \left[1 + B Vi \left(\frac{D_{32}}{D_o} \right)^{1/3} \right]^{3/5} \quad (14)$$

Eq. 14 is of exactly the same form as the correlation developed by Wang and Calabrese (1986) for stirred tanks. The empirical constants A and B will differ due to geometric factors contained in the definitions of We and Vi, differences in the spatial distribution of energy dissipation rate and possibly to differences in the breakage mechanism. Eq. 14 reduces to Eq. 1 in the limit of negligible viscous resistance to breakage (Vi→0).

The constants A and B can be obtained via linear least squares regression from a plot of $We(D_{32}/D_o)^{5/3}$ versus $Vi(D_{32}/D_o)^{1/3}$. Values of We and Vi for each experiment are given in Table 3. The result with all data points weighted equally is

$$\frac{D_{32}}{D_o} = 0.49\ We^{-3/5}\left[\ 1 + 1.38\ Vi\left(\frac{D_{32}}{D_o}\right)^{1/3}\ \right]^{3/5} \qquad (15)$$

The goodness of fit of Eq. 15 is shown in Figure 9. The correlation coefficient is 0.85. It should be noted that linear plots of this type tend to emphasize scatter in the data relative to the more commonly employed log-log plots (eg. Figure 10). It is seen that Eq. 15 provides a good fit to the data although some dependency on Re is apparent. There are several plausible explanations for the scatter in the data. Although unlikely, the mixer may not be long enough to insure an equilibrium suspension at its exit. There may be some residual effect of initial drop size particularly at low Re and high μ_d. Some Reynolds numbers may not be high enough to insure an inertial subrange. The steep mean velocity gradients close to the mixer surfaces or the coherent wake structures behind the individual elements may play some role in droplet dispersion. Such secondary hydrodynamic effects would cast suspicion on the use of Eq. 11 to describe the disruptive force acting on the drop.

In the inviscid limit (Vi → 0), Eq. 15 reduces to

$$\frac{D_{32}}{D_o} = 0.49\ We^{-3/5} \qquad (16)$$

Figure 9 shows that Eq. 15 tends to over predict the p-Xylene (μ_d' = 0.6 mPa·s) data so it is prudent to assess the applicability of Eq. 16 to surface force stabilized dispersions. Middleman obtained substantial data for dilute suspensions of low viscosity ($\mu_d \leq 1$ mPa·s) organics in water in two 21 element Kenics mixers of the pitch employed here. These and the p-Xylene data of this study are given on the Weber No. plot of Figure 10. Eq. 16 is seen to provide a good fit indicating that the data of this study are consistent with the equilibrium inviscid dispersed phase data of Middleman and that in the inviscid limit, Eq. 15

applies to a broader range of system variables than employed here.

While Middleman considered the Reynolds No. range of this study, most of his data were acquired at lower Re where the friction factor depends weakly upon Re (Figure 2). Therefore, Eq. 16 is not strictly valid and the inviscid limit of Eq. 13 should be used to correlate his data. This approach did not yield an improved fit. This is consistent with Middleman's argument that the dependency of f on Re and hence its effect on D_{32} is not sufficient to warrant its consideration.

Middleman also reported equilibrium data obtained in the same mixers for two slightly viscous organics dispersed in water (benzyl alcohol, 5 mPa·s and oleic acid, 26 mPa·s). These could not be correlated by Eq. 15. On Figure 9 the ordinate was up to 5 and 12 times larger than that of Eq. 15 for the benzyl alcohol and oleic acid data, respectively. The reason for this is not apparent. It could not be attributed to lower Reynolds No. Middleman reported that models containing a viscosity group as a second parameter failed with these data.

It should be noted that Middleman maintained holdup below 1% by volume. On the average his volume fractions, although dilute, were an order of magnitude greater than those employed here. Viscous drops are more likely to coalesce. His conclusion that the effect of Φ on D_{32} is negligible was based on $\mu_d = 0.6$ mPa·s and $\Phi \geq 0.01$. Figure 10 shows that Middleman's low viscosity data lie slightly above ours. It may be that some role is played by coalescence in the range $0.001 < \Phi < 0.01$ and that is becomes more pronounced as μ_d increases. A final consideration is that the oleic acid - water system exhibits complex interfacial phenomena whose role in liquid-liquid dispersion is difficult to quantify.

CORRELATION FOR FINAL DROP SIZE DISTRIBUTION

Consider a relative resistance to breakage defined as the ratio of cohesive to disruptive forces acting upon a drop. If

these forces are described as in Eq. 10 with τ_c given by Eq. 11 with 6, one finds that for a given drop size, the relative resistance to breakage increases with μ_d and σ and decreases with Re or $\bar{\varepsilon}$. As previously discussed, the broadness of the final drop size distribution follows the same trends so that this relative resistance becomes a measure of said. Therefore, it can be assumed that the probability density function which describes the distribution should depend only upon the relative resistance to breakage. Wang and Calabrese (1986) used exactly these arguments to show that, to a first approximation, the equilibrium drop size distribution produced in stirred tanks can be correlated by normalization with D_{32}. The argument for static mixers is the same and will not be repeated here. Instead we will simply seek a correlation of the form $F_v\ (D/D_{32})$.

Normalized drop size distributions for the 7 different dispersed phases are given at Re = 18000 in Figure 11. Normalized distributions at the four Reynolds numbers are given in Figure 12 for the 100 mPa·s silicone oil. The distributions are not quite normally distributed in volume displaying a slight sinusoidal variation. Middleman's (1974) distributions were also about normal but displayed a slight S shape. Except for scatter in the tails, normalization with D_{32} appears to provide an adequate correlation. Since the distributions are about normally distributed in volume, the normalized frequency can be approximated by (Wang and Calabrese, 1986).

$$F_v(X) = 0.5 \left[1 + \mathrm{ERF} \left(\frac{X - \bar{X}}{\sqrt{2}\ \sigma_v} \right) \right] \qquad (17)$$

where $X = D/D_{32}$ and $\bar{X}$ and σ_v are the volume weighted mean and standard deviation, respectively.

The data were fit to Eq. 17 via nonlinear least squares regression. On the average, 43 points in the range $0.002<F_v<0.99$ were used to describe each distribution. The result was

$$F_v\left(D/D_{32}\right) = 0.5\left[1 + \mathrm{ERF}\left(\frac{D/D_{32} - 1.12}{0.31\sqrt{2}}\right)\right] \qquad (18)$$

The root mean square deviation, based on the difference between the experimental and predicted value of F_v normalized by the experimental value, was 26%. The goodness of fit of Eq. 16 is visualized in Figures 11 and 12. The greatest deviations appear in the large size tail. The data of Figures 3 to 5 indicate that this may be a residual effect of the size distribution at the mixer entrance. If these deviations are solely due to initial drop size then, from the previous discussion, one would expect the degree of scatter to increase with increasing μ_d and decreasing Re. No such correlation was found. It is more likely that these deviations are inherent in the experimental technique. It is not reasonable to expect an accurate representation of the large size tail of the 3rd moment (volume) of the measured variable (diameter) from a sample population of 300 counts.

Middleman (1974) found that his equilibrium data were well correlated by Eq. 17 with $\bar{X} = 1.06$ and $\sigma_v = 0.25$. The data of this study show a slightly higher mean and a larger standard deviation. The increased broadness may be due to the higher dispersed phase viscosities employed here or may indeed be a residual effect of initial drop size. The latter is difficult to assess since Middleman did not provide information on his initial drop size. He also introduced the dispersed phase through a capillary tube. For stirred vessels, Wang and Calabrese (1986) reported that their correlation for cumulative volume frequency for a similar range of viscous dispersed phases was exactly the same as that of Chen and Middleman (1967) for inviscid drops. However, this conclusion was based upon a comparison of at least five times as much data as employed here.

ACKNOWLEDGEMENTS

This work was partially supported by grants from the Minta

Martin Fund for Aeronautical Research (University of Maryland) and the Center for Chemical Engineering, National Bureau of Standards (No. 70NANH0021). The authors wish to thank Mr. Carl Stoots who measured the friction factor data, and Dr. David Dickey and Chemineer-Kenics Inc. who provided the static mixer.

NOTATION

A,B = dimensionless empirical constants

$C_1,\ldots C_7$ = dimensionless empirical constants

D = drop size

D_{max} = maximum stable drop size

D_o = pipe on static mixer diameter

D_{32} = Sauter mean diameter

F_v = cumulative volume frequency

f = Fanning friction factor

L = length of mixer

L_e = length of single mixer element

n = number of drop counts

n_e = number of mixer elements

ΔP = pressure drop across mixer

Re = $\bar{V}\ D_o/\nu_c$, Reynolds No.

$\bar{V}$ = mean velocity of continuous phase in mixer based on cross-section of empty pipe

Vi = $(\mu_d\ \bar{V}\ /\sigma)\ (\rho_c/\rho_d)^{\frac{1}{2}}$, Viscosity Group on Capillary No.

We = $\rho_c\ \bar{V}^2 D_o/\sigma$, Weber No.

X = D/D_{32}, normalized drop diameter

$\bar{X}$ = volume weighted mean of X

Greek Letters

α = Kolmogorov constant

ϵ = local energy dissipation rate per unit mass

$\bar{\epsilon}$ = mean energy dissipation rate per unit mass

$\bar{\eta}$ = Kolmogorov microscale based on mean energy dissipation rate

μ_d = viscosity of dispersed phase

μ_d' = nominal dispersed phase viscosity

ν_c = kinematic viscosity of continuous phase

ρ_c = density of continous phase

ρ_d = density of dispersed phase

σ = interfacial tension

σ_v = volume weighted standard deviation of X

τ_c = turbulent disruptive force per unit area acting on drop

Φ = holdup or volume fraction of dispersed phase

LITERATURE CITED

Al Taweel, A.M. and L.D. Walker, "Liquid Dispersion in Static In-Line Mixers", Can. J. Chem. Eng., 61, 527-533 (1983).

Bird, R.B., W.E. Stewart and E.N. Lightfoot, Transport Phenomena, John Wiley and Sons, New York (1960).

Calabrese, R.V., T.P.K. Chang and P.T. Dang, "Drop Breakup in Turbulent Stirred Tank Contactors, Part I: Effect of Dispersed Phase Viscosity", AIChE J., 32, 657-666 (1986).

Chen, S.J. and D.R. Libby, "Gas-Liquid and Liquid-Liquid Dispersion in a Kenics Mixer", AIChE 71st Annual Meeting, Miami, Nov. (1978).

Chen, H.T. and S. Middleman, "Drop Size Distribution in Agitated Liquid-Liquid Systems, AIChE J., 13, 989-995 (1967).

Davies, J.T., "Drop Sizes of Emulsions Related to Turbulent Energy Dissipation Rates", Chem. Eng. Sci., 40, 839-842 (1985).

Hinze, J.O., "Fundamentals of the Hydrodynamic Mechanism of Splitting in Dispersion Processes", AIChE J., 1, 289-295 (1955).

Hughmark, G.A., "Drop Breakup in Turbulent Pipe Flow", AIChE J., 17, 1000 (1971).

Kolmogorov, A.N., "The Breakup of Droplets in a Turbulent Stream", Dok. Akad. Nauk., 66, 825-828 (1949).

Middleman, S., "Drop Size Distributions Produced by Turbulent Pipe Flow of Immiscible Fluids through a Static Mixer", Ind. Eng. Chem. Process Des. & Dev., 13, 78-83 (1974).

Paul, H.I. and C.A. Sleicher, Jr., "The Maximum Stable Drop Size in Turbulent Flow: Effect of Pipe Diameter", Chem. Eng. Sci., 20, 57-59 (1965).

Shinnar, R., "On the Behavior of Liquid Dispersions in Mixing Vessels", J. Fluid Mech., 10, 259-275 (1961).

Sleicher, Jr., C.A. "Maximum Stable Drop Size in Turbulent Flow", AIChE J., 8, 471-477 (1962).

Tavlarides, L.L. and M. Stamatoudis, "The Analysis of Interphase Reactions and Mass Transfer in Liquid-Liquid Dispersions", Advances in Chemical Engineering, 11, 199-273 (1981).

Wang, C.Y. and R.V. Calabrese, "Drop Breakup in Turbulent Stirred Tank Contactors, Part II: Relative Influence of Viscosity and Interfacial Tension", AIChE J., 32, 667-676 (1986).

Table 1: Physical Properties of Dispersed Phases

Dispersed Phase	Nominal Viscosity μ_d' (mPa·s)	Temperature °C	Viscosity μ_d (mPa·s)	Density ρ_d (g·cm^{-3})	Interfacial* Tension σ (mN·m^{-1})
Silicone Oil	20	21	19.6	.947	37.4
		22	19.4	.946	37.4
	50	20	51.8	.963	37.4
		22	49.9	.961	37.4
		23	49.0	.960	37.4
	100	22	103	.962	37.4
	200	21	204	.967	37.4
		22	201	.966	37.4
Paraffin Oil	45	23	46.1	.853	41.6
		24	43.0	.852	41.6
	150	23	161	.876	41.6
		24	151	.875	41.6
		25	141	.874	41.6
p-Xylene	0.6	21	.64	.857	31.8
		22	.63	.856	31.8

* with water (continuous phase)

Table 2: Experimentally Determined Initial and Final Drop Diameters

Dispersed Phase	Nominal Dispersed Phase Viscosity μ_d' (mPa·s)	Reynolds Number 12,000 D_{32} - µm		15,000 D_{32} - µm		18,000 D_{32} - µm		21,000 D_{32} - µm	
		Initial	Final	Initial	Final	Initial	Final	Initial	Final
Silicone Oil	20	1890	483	1431	309	1380	245	1098	183
	50	1932	547	1548	380	1475	295	1254	240
	100	2355	704	1877	468	1718	355	1510	300
	200	2101	784	1788	550	1689	411	1490	370
Paraffin Oil	45	2177	658	1852	484	1533	405	1497	290
	150	2716	920	2422	614	2328	509	1951	393
p-Xylene	0.6	1765	286	1239	204	942	161	901	106

Table 3: Weber No. and Viscosity Group

Dispersed Phase	Nominal Dispersed Phase Viscosity μ_d' (mPa·s)	Reynolds Number 12,000		15,000		18,000		21,000	
		Vi	We	Vi	We	Vi	We	Vi	We
Silicone Oil	20	.321	185	.416	303	.499	436	.563	566
	50	.820	195	1.12	318	1.23	416	1.38	541
	100	1.69	185	2.11	289	2.53	416	2.96	566
	200	3.29	185	4.29	303	5.14	436	5.75	566
Paraffin Oil	45	.643	151	.861	247	1.06	356	1.13	463
	150	2.03	144	3.03	247	3.05	325	3.90	463
p-Xylene	0.6	.0133	228	.0166	356	.0193	500	.0225	665

FIGURE CAPTIONS

Figure 1 Schematic diagram of experimental facility

Figure 2 Fanning friction factor for Kenics static mixer. $n_e = 21$; $D_o = 1.91$ cm; $L_e/D_o = 1.5$.

Figure 3 Drop size distribution at entrance and exit of mixer for p-Xylene dispersed in water. $\mu_d' = 0.6$ mPa·s; $\sigma = 31.8$ mN·m^{-1}.

Figure 4 Drop size distribution at entrance and exit of mixer for 50 mPa·s silicone oil dispersed in water. $\mu_d' = 50$ mPa·s; $\sigma = 37.4$ mN·m^{-1}.

Figure 5 Drop size distributions at entrance and exit of mixer for the more viscous paraffin oil dispersed in water. $\mu_d' = 150$ mPa·s; $\sigma = 41.6$ mN·m^{-1}.

Figure 6 Final Sauter mean diameter versus dispersed phase viscosity as a function of Reynolds No. for silicone oil - water dispersions. $\sigma = 37.4$ mN·m^{-1}.

Figure 7 Relationship between maximum stable drop size and Sauter mean diameter at exit of mixer.

Figure 8 Effect of dispersed phase viscosity on final drop size distribution. Paraffin oil-water dispersions; Re = 12000; $\sigma = 41.6$ mN·m^{-1}.

Figure 9 Correlation for equilibrium mean drop size.

Figure 10 Comparison of Eq. 16 with data for inviscid dispersed phases. For all data the continuous phase is water. Except for p-Xylene all data are those of Middleman (1974).

Figure 11 Similarity of normalized volume distribution at mixer exit for constant conditions of agitation. Re = 18000.

Figure 12 Similarity of normalized volume distribution at mixer exit for constant physical properties. Silicone oil-water dispersions; $\mu_d' = 100$ mPa·s; $\sigma = 37.4$ mN·m^{-1}.

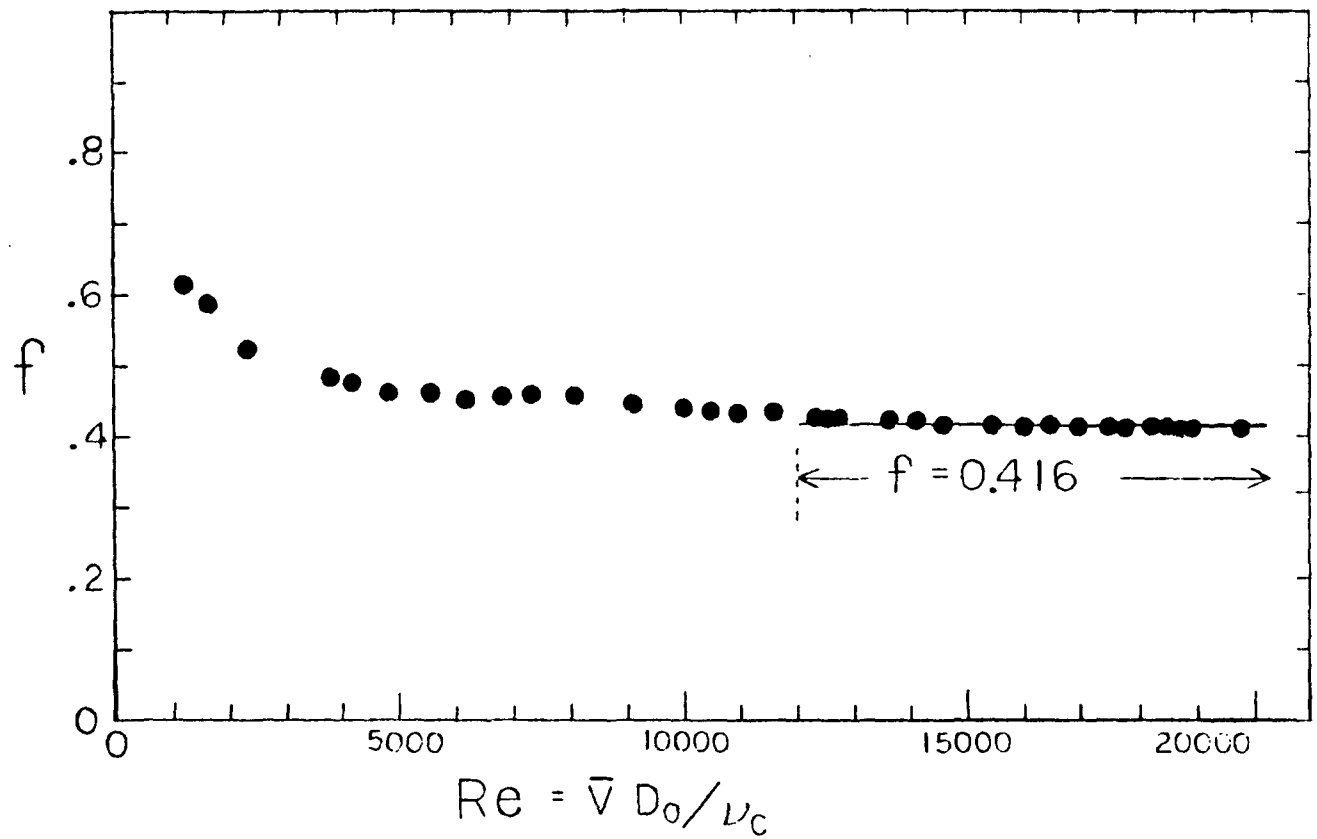

Figure 2

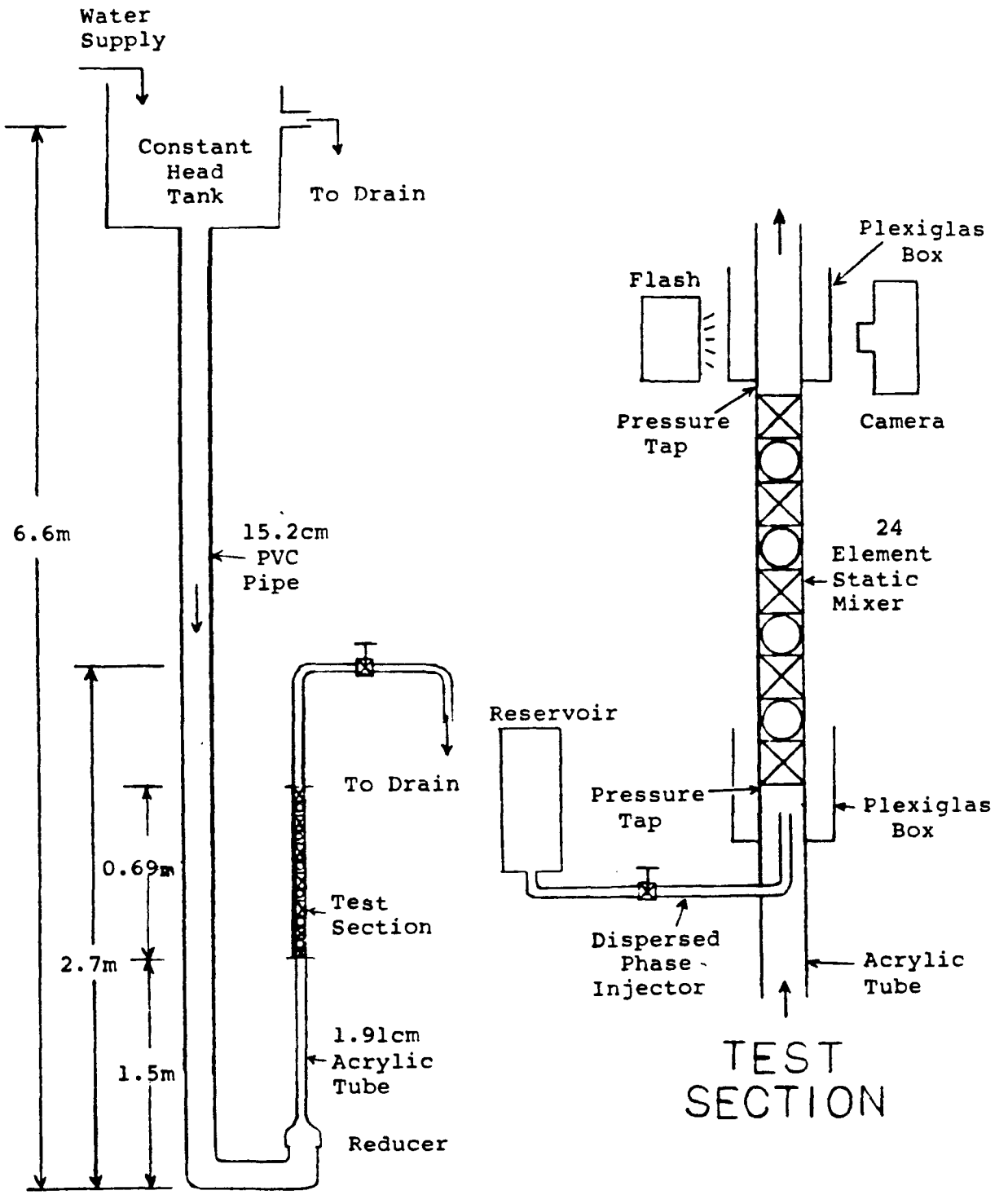
Water Supply
Constant Head Tank
To Drain
6.6m
15.2cm PVC Pipe
To Drain
0.69m
Test Section
2.7m
1.91cm Acrylic Tube
1.5m
Reducer
Flash
Plexiglas Box
Pressure Tap
Camera
24 Element Static Mixer
Reservoir
Pressure Tap
Plexiglas Box
Dispersed Phase Injector
Acrylic Tube
TEST SECTION

Figure 1

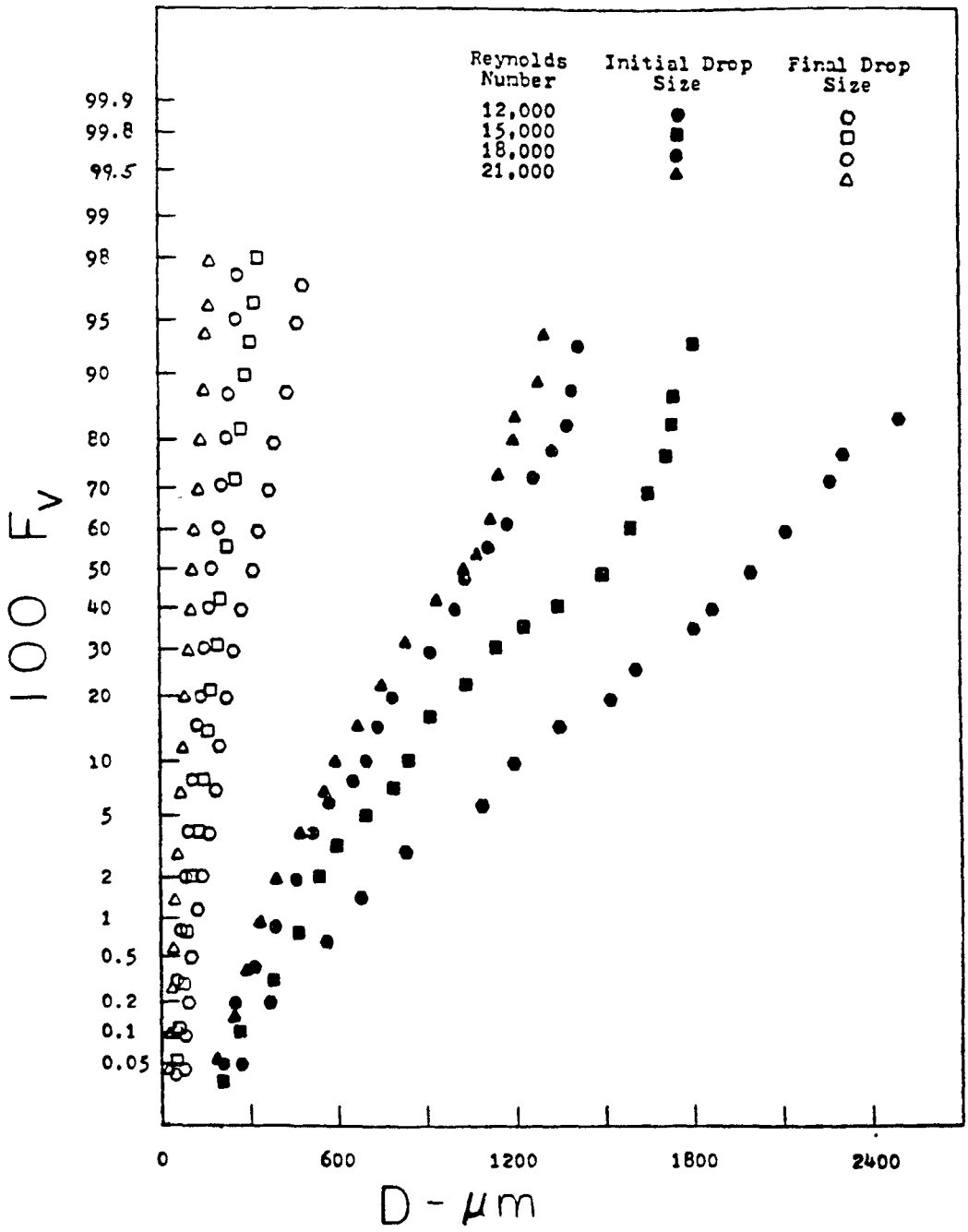
Reynolds Number
Initial Drop Size
Final Drop Size
12,000
15,000
18,000
21,000
100 F_v
99.9
99.8
99.5
99
98
95
90
80
70
60
50
40
30
20
10
5
2
1
0.5
0.2
0.1
0.05
0
600
1200
1800
2400
D - μm

Figure 3

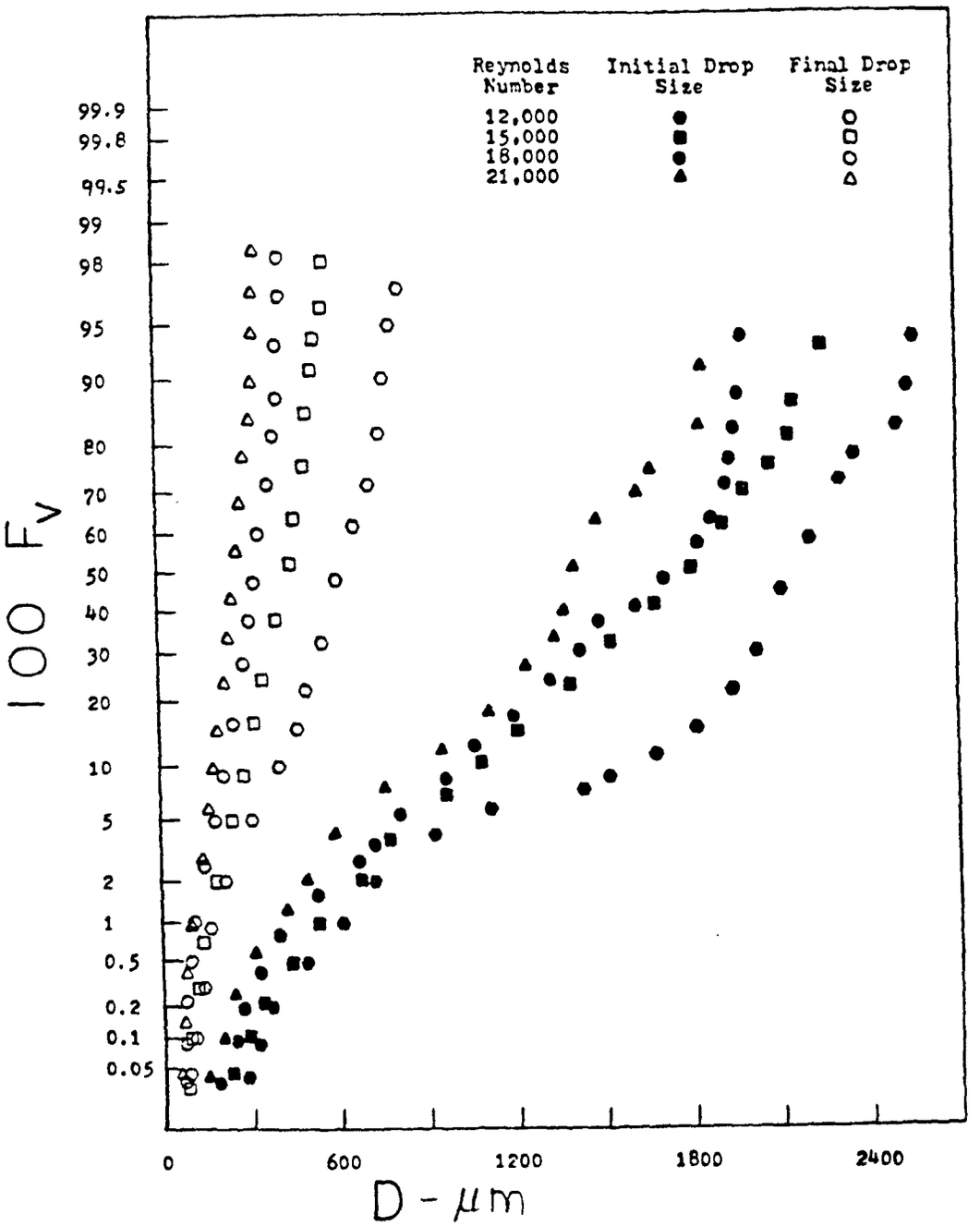
Reynolds Number
Initial Drop Size
Final Drop Size
12,000
15,000
18,000
21,000
100 Fv
99.9
99.8
99.5
99
98
95
90
80
70
60
50
40
30
20
10
5
2
1
0.5
0.2
0.1
0.05
0
600
1200
1800
2400
D - μm

Figure 4

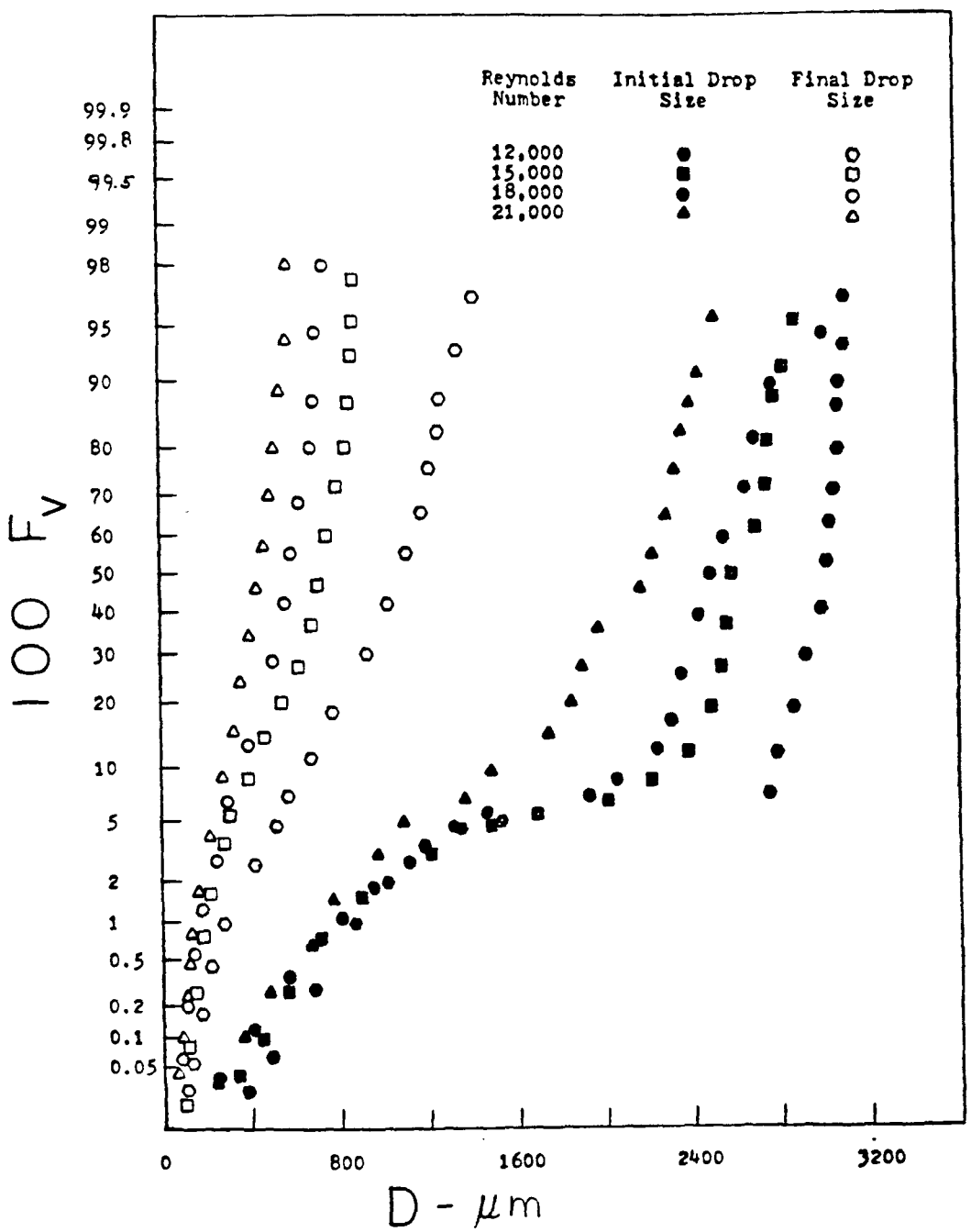
Reynolds Number
Initial Drop Size
Final Drop Size
12,000
15,000
18,000
21,000
99.9
99.8
99.5
99
98
95
90
80
70
60
50
40
30
20
10
5
2
1
0.5
0.2
0.1
0.05
100 Fv
0
800
1600
2400
3200
D - μm

Figure 5

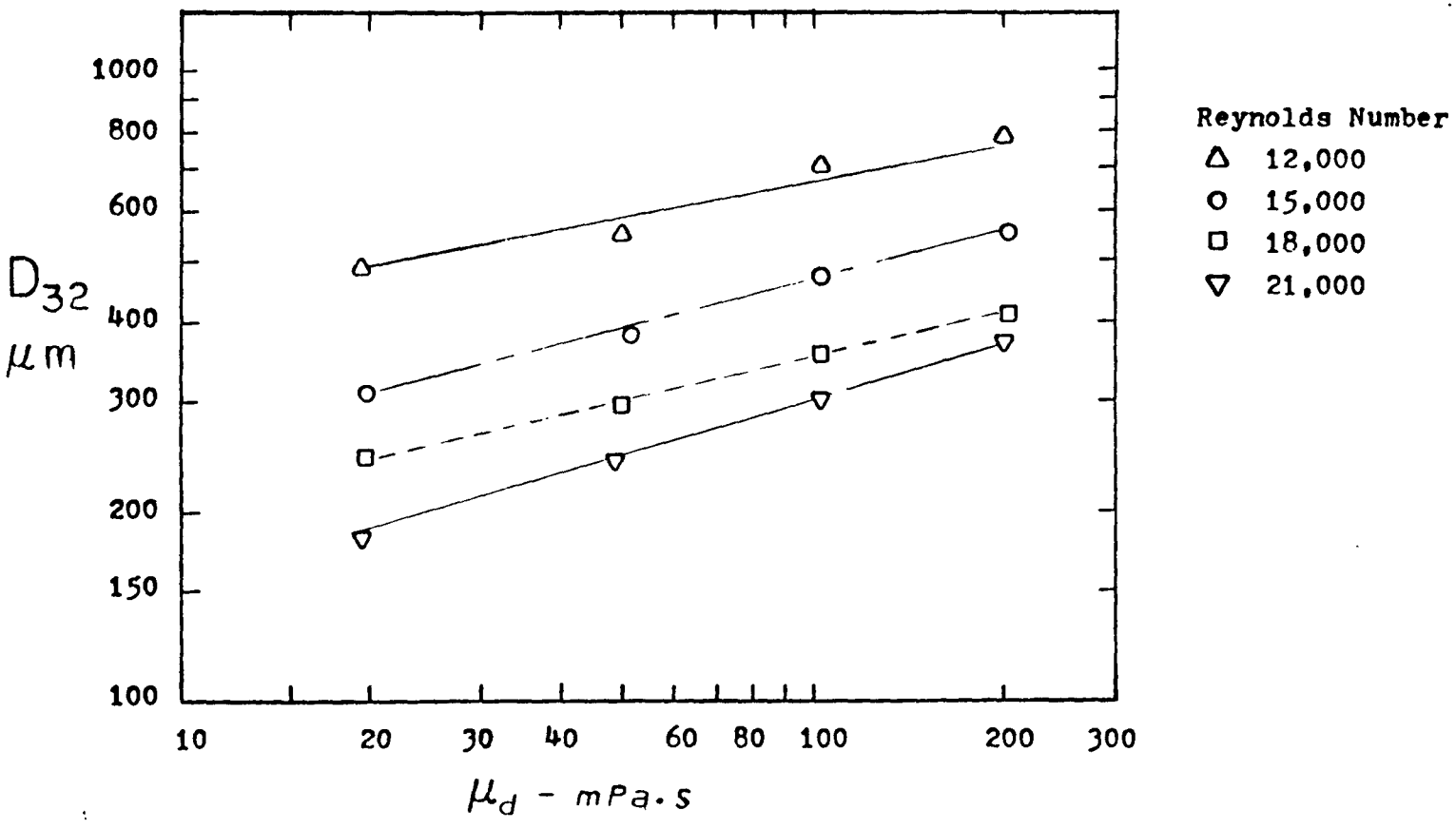
1000
800
600
400
300
200
150
100
D_{32}
μm
10
20
30
40
60
80
100
200
300
μ_d - mPa.s
Reynolds Number
12,000
15,000
18,000
21,000

Figure 6

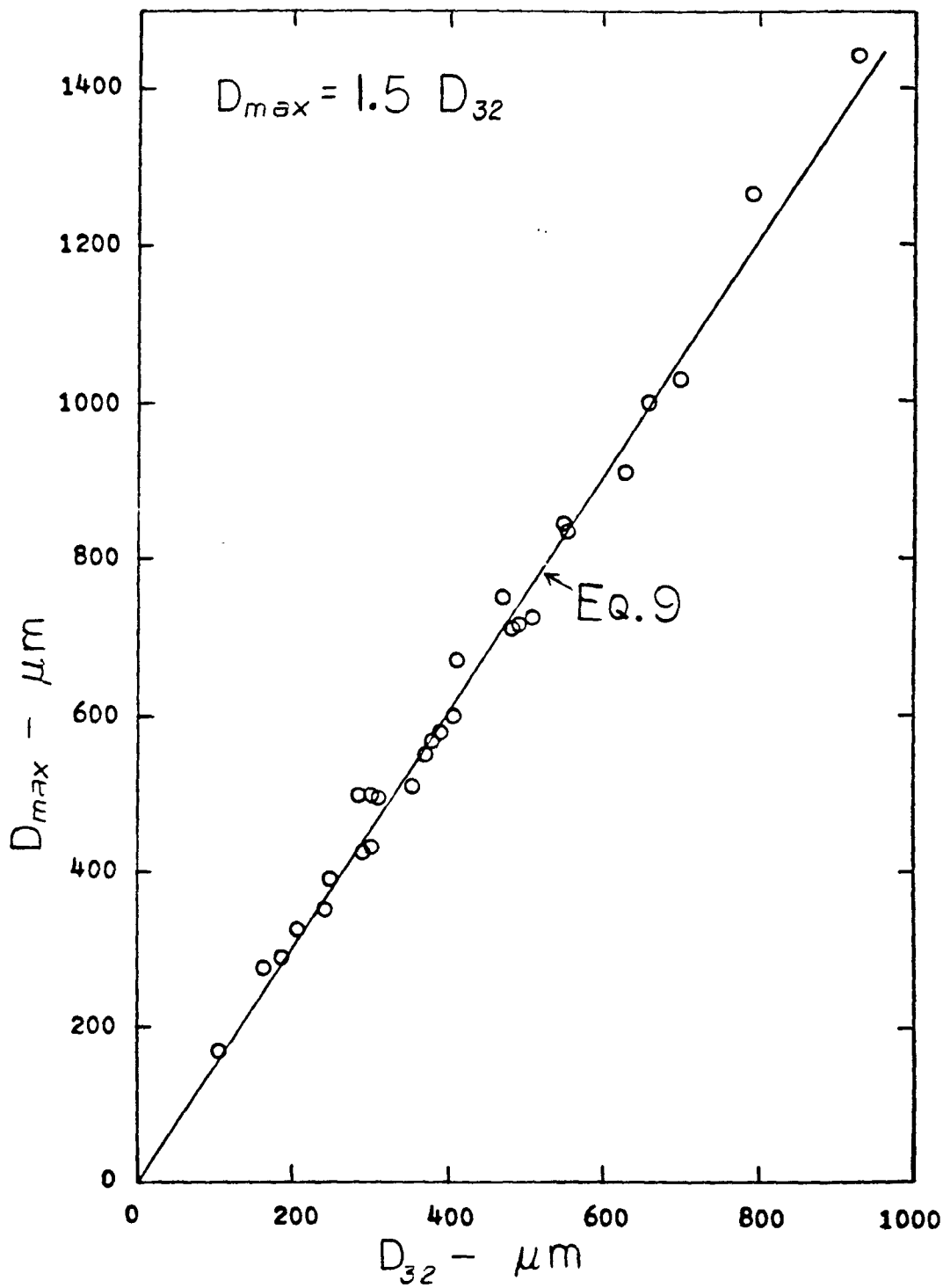

Figure 7

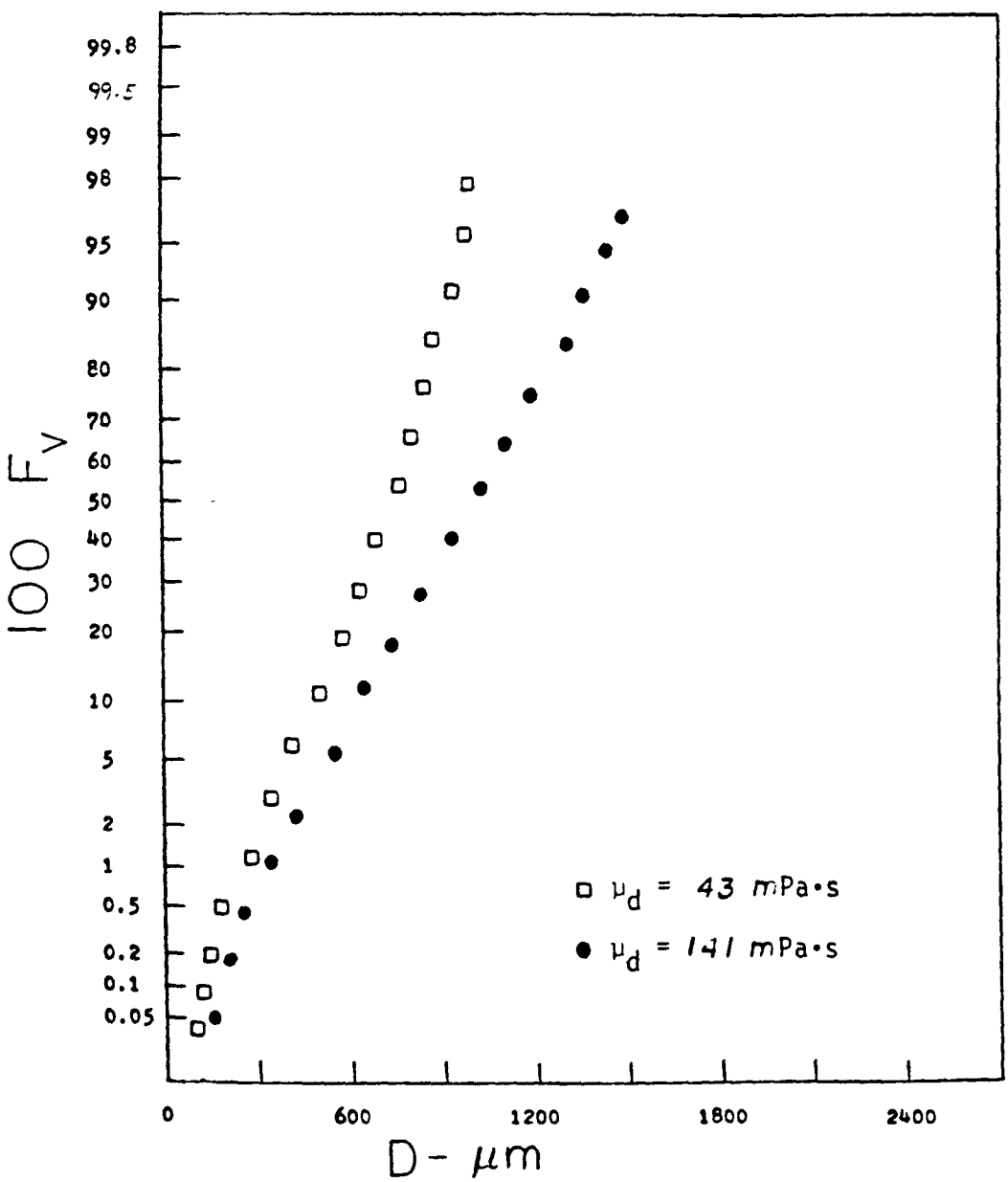
99.8
99.5
99
98
95
90
80
70
60
50
40
30
20
10
5
2
1
0.5
0.2
0.1
0.05
100 F_v
0
600
1200
1800
2400
D - μm
□ μ_d = 43 mPa·s
● μ_d = 141 mPa·s

Figure 8

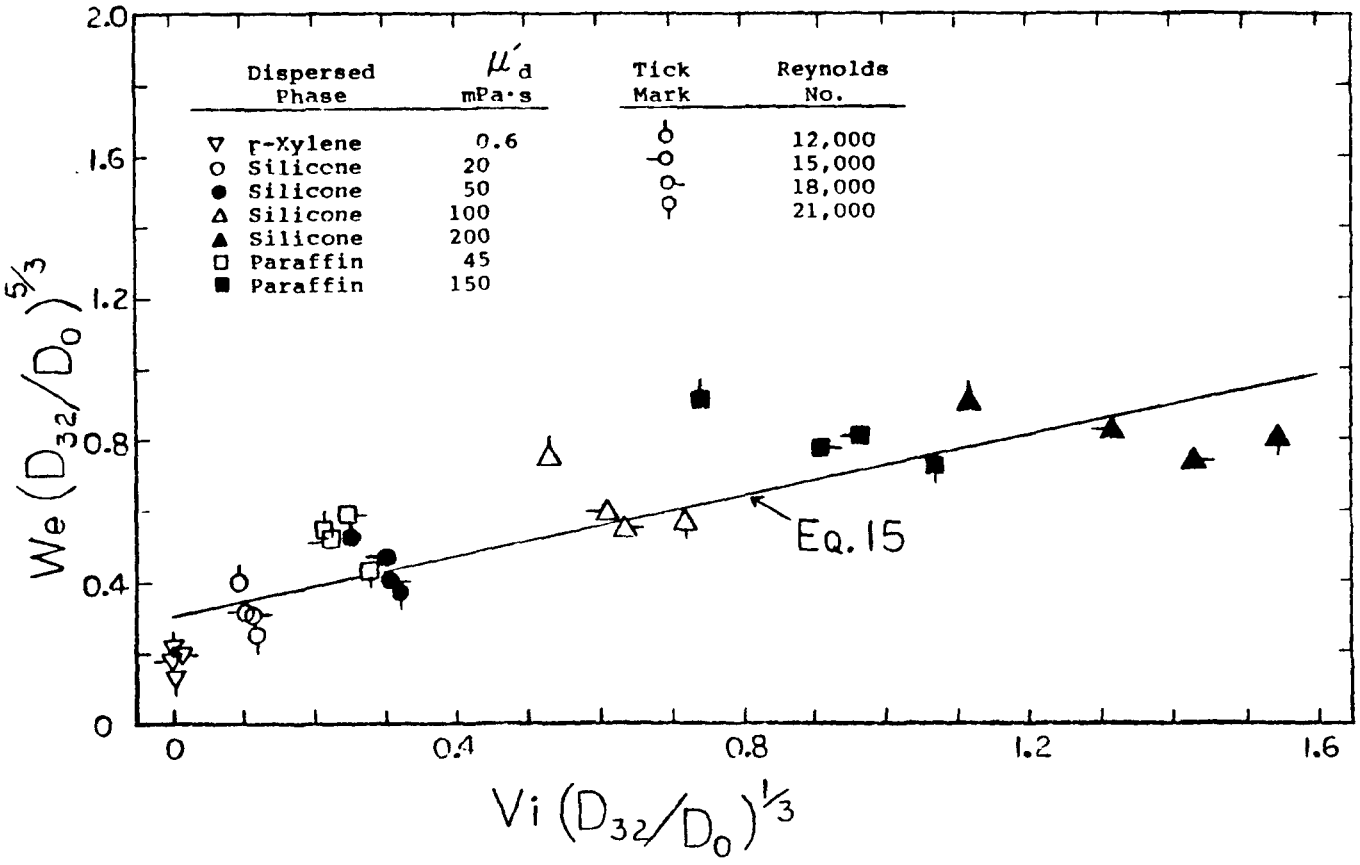
Dispersed Phase
μ'd mPa·s
Tick Mark
Reynolds No.
p-Xylene 0.6 12,000
Silicone 20 15,000
Silicone 50 18,000
Silicone 100 21,000
Silicone 200
Paraffin 45
Paraffin 150
Eq. 15
We (D32/D0)5/3
Vi (D32/D0)1/3
0
0.4
0.8
1.2
1.6
2.0

Figure 9

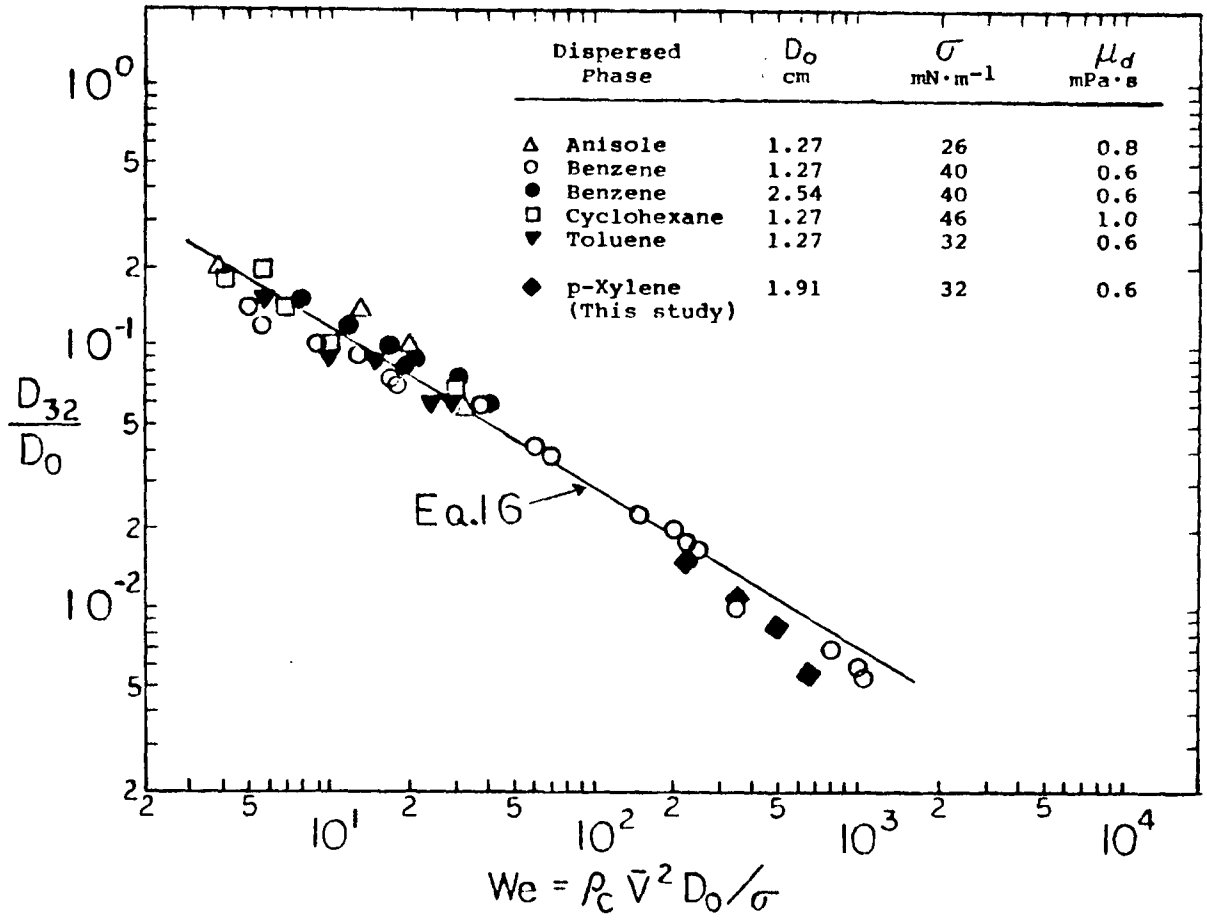
Dispersed Phase
D_o cm
σ mN·m^{-1}
μ_d mPa·s
Anisole 1.27 26 0.8
Benzene 1.27 40 0.6
Benzene 2.54 40 0.6
Cyclohexane 1.27 46 1.0
Toluene 1.27 32 0.6
p-Xylene (This study) 1.91 32 0.6
Eq.16
$\frac{D_{32}}{D_0}$
$We = \rho_c \bar{V}^2 D_0/\sigma$

Figure 10

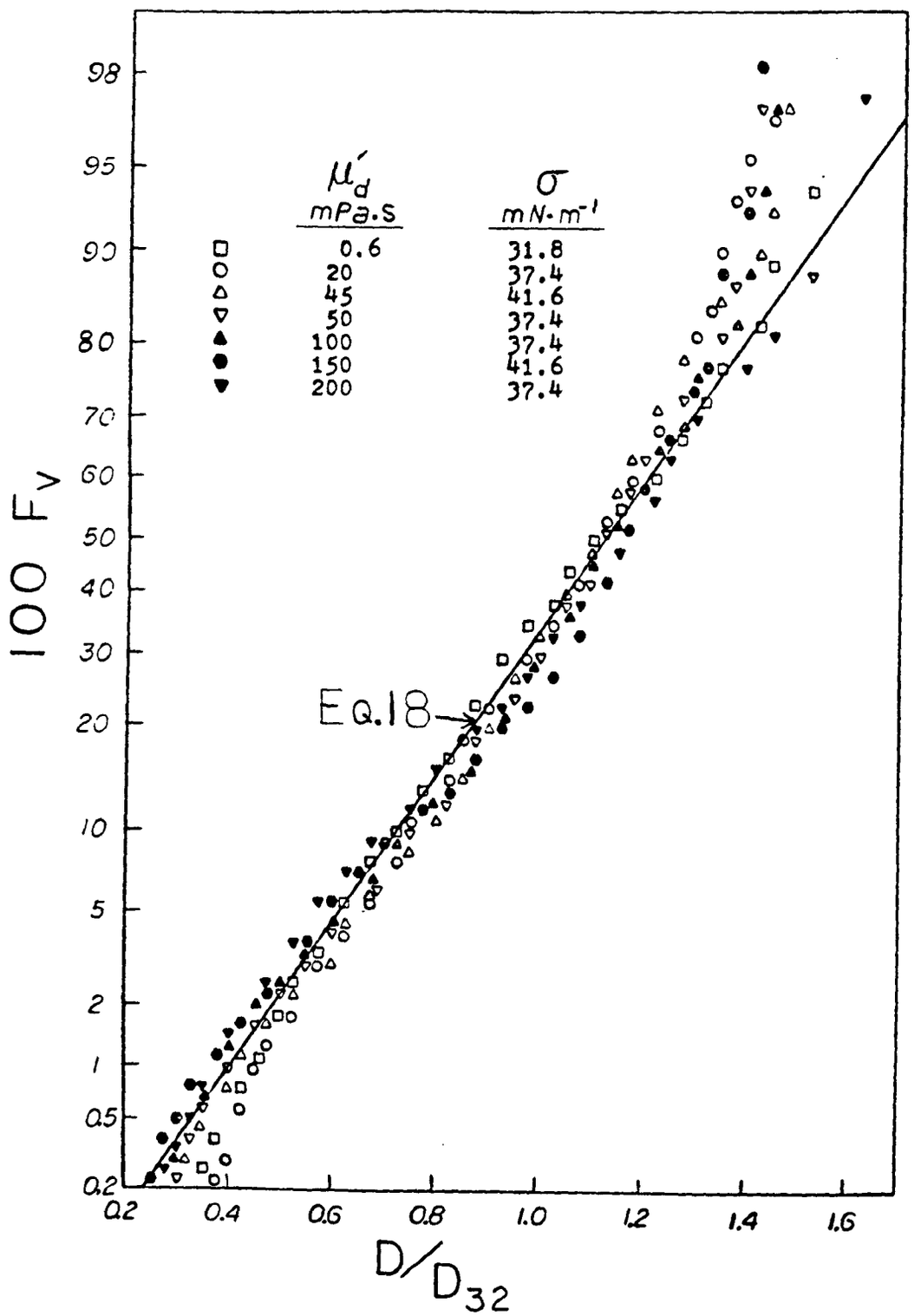
100 F_V
98
95
90
80
70
60
50
40
30
20
10
5
2
1
0.5
0.2
μ'_d mPa.S
σ mN·m^{-1}
0.6 31.8
20 37.4
45 41.6
50 37.4
100 37.4
150 41.6
200 37.4
Eq.18
0.2
0.4
0.6
0.8
1.0
1.2
1.4
1.6
D/D_{32}

Figure 11

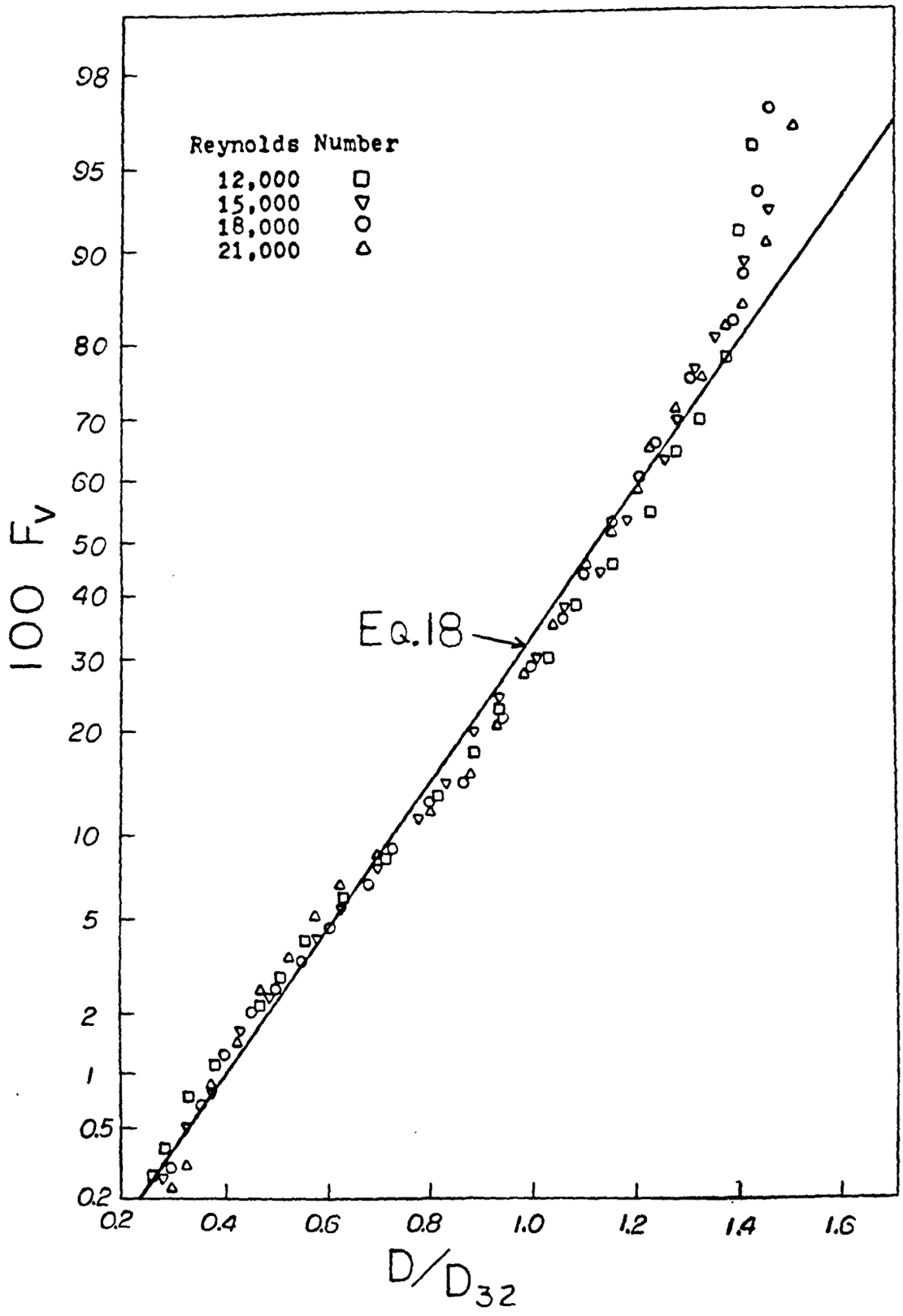
Reynolds Number
12,000
15,000
18,000
21,000
Eq.18
100 F_v
98
95
90
80
70
60
50
40
30
20
10
5
2
1
0.5
0.2
0.2
0.4
0.6
0.8
1.0
1.2
1.4
1.6
D/D_{32}

Figure 12